Agglomeration Beyond Productivity:
Economic Organization and Resilience to Natural Disasters

Haeseong Park*

2026-07-13

Abstract

This paper examines how differences in economic structure shape the short-run economic impacts of natural disasters on cities. Using wind strength to proxy disaster intensity and electricity consumption to measure economic activity, I show that natural disasters reduce aggregate economic activity by 3 percent at the metropolitan statistical area (MSA) level under average agglomeration conditions.I find substantial heterogeneity in disaster impacts across three dimensions of urban economic structure: labor market concentration, transportation network centralization, and local trade linkages. Higher industry concentration amplifies losses by more than twofold, whereas centralized road networks and greater internal goods sourcing mitigate them, with the latter reducing losses by nearly half. Using granular industry specialization profiles, I find that increases in specialization in non-tradable local industries magnify the adverse economic effects of natural disasters.

Cities overwhelmingly concentrate economic activity. In the United States, metropolitan statistical areas (MSAs) account for the vast majority of employer establishments and population[1], making cities the primary locus of production, employment, and innovation. This geographic concentration has long motivated research on agglomeration economies, which explain how the spatial concentration of economic activity generates greater productivity gains. Beyond the early focus on industrial concentration, it has expanded to

*University of Colorado Boulder

[1]In 2023, MSAs contained approximately 7.9 million of the nation's 8.4 million employer establishments, accounting for nearly 95 percent of all employer establishments in the United States. Likewise, approximately 86 percent of the U.S. population, 294 million people, resided in MSAs as of July 1, 2024.

encompass more granular labor-market composition, highlighting the role of specialization in producer service occupations in driving recent urban economic growth. It has also broadened to examine the underlying structures of interconnected economic linkages, including transportation networks that facilitate interactions and trade linkages that connect firms and markets[2]. Together, these advances suggest that agglomeration is not a one-dimensional phenomenon defined solely by the intensity of geographic concentration. Rather, urban economic performance depends on multiple, interconnected dimensions of economic organization, including labor-market composition, goods sourcing networks, and transportation connectivity. This increasingly multidimensional view of agglomeration raises a broader question: if urban economies differ not only in the extent of geographic concentration but also in how economic activity is organized, is productivity alone sufficient for evaluating alternative forms of urban organization?

This increasingly multidimensional understanding of agglomeration nevertheless rests largely on evidence from ordinary economic conditions, where these dimensions have been evaluated primarily through their contributions to productivity. Under these conditions, the mechanisms generating agglomeration economies remain largely intact, making productivity the primary lens through which alternative forms of urban organization are evaluated. Yet cities are periodically exposed to natural disasters, and much less is known about how these organizational dimensions shape economic outcomes when the functioning of urban economies is disrupted. Indeed, the fact that cities with similar levels of geographic concentration often experience markedly different economic losses suggests that differences in the configuration of these dimensions constitute an important

[2]Regarding the labor market concentration, Glaeser et al. (2004)(32) and Behrens et al. (2014)(7) emphasize the fundamental role of skilled human capital in city development. Wage premia arising from firm competition in cities attract additional workers, further expanding urban areas and reinforcing agglomeration economies. Duranton et al. (2001)(23) illustrate the dynamics of city-level specialization, showing that innovation tends to emerge in diversified cities, while mass production often relocates to more specialized cities with lower production costs. In this paper, city diversity is measured as the inverse of the Herfindahl index based on sectoral employment shares within each city.

Regarding transportation infrastructure, Duranton et al. (2012)(24) find that a greater initial stock of highways leads to higher long-run employment and faster economic growth at the city level. Similarly, Baum-Snow (2007)(**?**) shows that the expansion of the interstate highway system contributed substantially to urban decentralization in the United States between 1950 and 1990.

From the perspective of economic geography and trade, Marin et al. (2021)(44) document that export activity is disproportionately concentrated in larger cities, implying greater potential gains from trade at the urban level and reciprocal benefits for city development.

Furthermore, three agglomeration forces are also closely interconnected. For example, Marin et al. (2021)(44) show that active trade shifts labor supply toward larger cities, while Duranton et al. (2014)(25) find that interstate highways increase the overall volume of exports across U.S. cities, though they have little effect on total export value.

source of heterogeneity in urban resilience. As natural disasters become increasingly frequent, as evidenced by the roughly fourfold increase in billion-dollar disasters since the 1980s,[3] understanding this overlooked side of agglomeration becomes increasingly important. Rather than asking only which forms of urban organization promote productivity, this paper broadens the evaluation of agglomeration by examining how alternative forms of urban structure contribute to heterogeneity in urban resilience.

This paper investigates whether differences in the organization of labor markets, transportation networks, and trade activity shape the economic resilience of cities to natural disasters. Specifically, it investigates whether these organizational dimensions moderate the relationship between geographic concentration and disaster damages, either strengthening or weakening the economic consequences of concentration. More broadly, the paper asks under what organizational conditions agglomeration remains an asset rather than becoming a source of vulnerability, extending the evaluation of agglomeration beyond productivity to resilience. It considers three organizational dimensions of cities: labor-market composition, transportation network structure, and trade linkages. A city's industrial base may be be concentrated in a narrow set of industries, its transportation network may depend on a limited number of critical road segments, and its goods sourcing may rely primarily on local suppliers rather than geographically diversified trade linkages. Together, these dimensions govern how workers, goods, and transportation are organized within cities, thereby shaping how geographic concentration translates differently into economic losses following natural disasters.

The heterogeneous effects of urban structural dimensions, combined with the inherently unpredictable and transient nature of natural disasters, necessitate a carefully designed empirical strategy. Thus, with a local projection difference-in-differences (LP-DiD) framework developed by Dube et al. (2023)(22) and Jordà et al. (2025)(40), I construct a monthly panel of U.S. MSAs to examine how urban organization shapes resilience to natural disasters and estimate dynamic responses to disaster exposure. Because natural disasters are temporary events that can repeatedly affect the same city over time, the LP-DiD framework accommodates intermittent treatment while constructing appropriate control cities that remain unexposed during each event window. I measure local economic activity using monthly commercial and industrial electricity consumption at

[3] NOAA National Centers for Environmental Information, U.S. Billion-Dollar Weather and Climate Disasters (2024), `https://www.ncei.noaa.gov/access/billions/`, DOI: 10.25921/stkw-7w73.

the MSA level, following Cicala (2023)(17). Disaster exposure is measured using average monthly wind intensity, with treatment defined as wind speeds corresponding to hurricane Category 2 or higher.

This paper yields three main findings. First, major natural disasters have substantial short-run economic consequences. Holding the three organizational dimensions at their mean levels, a high-wind disaster of at least Saffir–Simpson Category 2 intensity reduces monthly economic activity, measured by commercial and industrial electricity consumption, by approximately 3 percent relative to pre-disaster levels. Consistent with this decline, employment growth falls by roughly 600 hires relative to the preceding three months, indicating substantial disruptions to local production activity.

Second, the average effects mask substantial heterogeneity across cities arising from differences in urban organization. Exploiting variation in labor-market composition, transportation network structure, and trade linkages across MSAs, I show that these organizational dimensions shape disaster resilience in fundamentally different ways. Labor-market concentration amplifies economic disruptions, whereas transportation network centralization and stronger intra-city goods-sourcing capacity enhance post-disaster economic resilience. More specifically, a one-standard-deviation increase in industrial composition concentration increases the decline in economic activity from 3 percent to approximately 7.3 percent. Put differently, when employment is concentrated in a narrow set of industries rather than distributed across a more diversified labor market, the short-run economic disruptions from natural disasters become roughly 2.5 times larger than the baseline effect. In contrast, a one standard deviation increase in road network centralization, measured by the extent to which a small number of road segments play a dominant role in connecting locations within a city, causes the baseline economic losses associated with a disaster event to largely disappear. Similarly, a one standard deviation increase in intra-city goods-sourcing capacity, which captures the extent to which a city's logistics system relies on internally sourced goods, reduces disaster-related damages by approximately 44 percent. Taken together, these findings underscore the heterogeneous roles of urban economic structures in shaping disaster resilience, with different forms of concentration either amplifying or mitigating economic damages.

Finally, I find that the vulnerability associated with labor-market concentration depends critically on the industries in which cities specialize. I distinguish five broad industry groups, Retail, Utilities, and Construction (RUC); Business Services (BS); Health and Education (HE); Manufacturing (M); and Accommodation, Wholesale Trade, and Transportation (ATT), and find that specialization in RUC and Manufacturing disproportionately amplifies disaster damages. A one-unit increase in specialization intensity amplifies economic losses by approximately 1.5 times in RUC and 2.2 times in Manufacturing. These findings suggest that the resilience consequences of industrial concentration depend not only on its intensity but also on the industry group in which concentration occurs, with important implications for evaluating urban specialization and ongoing structural transformation under increasing disaster risk. Taken together, these findings suggest that the benefits of agglomeration cannot be evaluated solely through productivity, as organizational structures that perform well under normal conditions may be considerably more vulnerable to natural disasters.

The main contribution of this paper is to identify the distinct roles that different dimensions of urban economic structure play in shaping the economic impacts of natural disasters. From the perspective of industrial composition, natural disasters provide a setting in which the long-standing debate between specialization and diversification appears to favor diversification, as less diversified local economies experience more severe economic damages (Heblich et al. (2025)(35); Moretti et al. (2024)(52); Combes et al. (2012)(18); Duranton et al. (2001)(23); Glaeser et al. (1992)(33); Jacobs (1969)(38); Marshall (1890)(45)). The mitigating effects of more centralized road networks may reflect the faster restoration of critical transportation infrastructure (Miyauchi et al. (2025)(49); Bergantino et al. (2024)(8); Allen et al. (2022)(1); Tyndall (2021)(60); Fajgelbaum et al. (2020)(28); Duranton et al. (2012)(24)), while stronger intra-city goods-sourcing capacity may operate through thicker buyer–supplier linkages that help sustain economic activity in the aftermath of a disaster (Miyauchi (2024)(48); Marin et al. (2021)(44); Duranton et al. (2014)(25)).

Another contribution of this paper is to examine heterogeneity in disaster resilience across industry groups by highlighting the role of industry-specific specialization, an aspect that has received little attention in the existing literature. While the importance of non-cognitive and non-routine intensive industries in promoting urban growth is well established (Monte et al.(2023)(50); Eckert et al.(2022)(27); Hsieh et al. (2023)(37); Jarosch et al.(2021)(39); Rossi-Hansberg et al.(2021) (54); Fajgelbaum et al. (2020)(28);

Rossi-Hansberg et al(2019)(55)), far less is known about whether specialization in particular industry groups shapes resilience to natural disasters. This paper fills that gap by showing that specialization in Retail, Utilities, and Construction (RUC) and Manufacturing significantly amplifies disaster-related economic losses.

The remainder of the paper is organized as follows. The next section describes the construction of the monthly economic activity proxy, the measure of natural disaster intensity, and the three measures of urban economic structure. Section II provides the empirical context for the research design, with particular attention to the LP-DiD framework. Section III presents the main empirical results and a series of robustness checks. Section IV investigates heterogeneity in disaster resilience across industry groups. Section V concludes.

I Data

I.I Electricity Consumption Loads

I use monthly electricity consumption as a proxy for overall economic activity at the MSA level, following Cicala (2023) (17). Alternative measures, such as monthly wage bills or employment from the Quarterly Census of Employment and Wages (QCEW), are less suitable for capturing the short-run economic effects of natural disasters. First, wage bills are unlikely to exhibit substantial variation at a monthly frequency because wages tend to adjust slowly and are typically determined over longer horizons. Indeed, even during prolonged economic downturns, labor market adjustments have historically occurred primarily through reductions in employment rather than cuts in wages. As a result, monthly wage bills may not adequately capture the immediate economic disruptions caused by natural disasters.

To more accurately capture economic activity using electricity data, I restrict the measure to commercial and industrial electricity consumption and exclude electricity used for residential and transportation purposes. The data are drawn from the U.S. Energy Information Administration's (EIA) Form 861M, the Monthly Electric Power Industry Report, and Form 861, the Annual Electric Power Industry Report. Electricity sales data are available at the utility-month level and a utility's service territory frequently spans multiple counties and may extend across multiple MSAs and state boundaries.

Consequently, utility service territories do not generally align with MSA boundaries, requiring the construction of MSA-level measures from utility-level electricity sales data. Figure 1 presents the geographic scope of utilities varies substantially across states. On average, a single utility within one state serves approximately 2.7 MSAs, with a median of 2.1 and a range from 0.3 to 9.5 MSAs. Thus, one utility within a state can cover multiple MSAs.

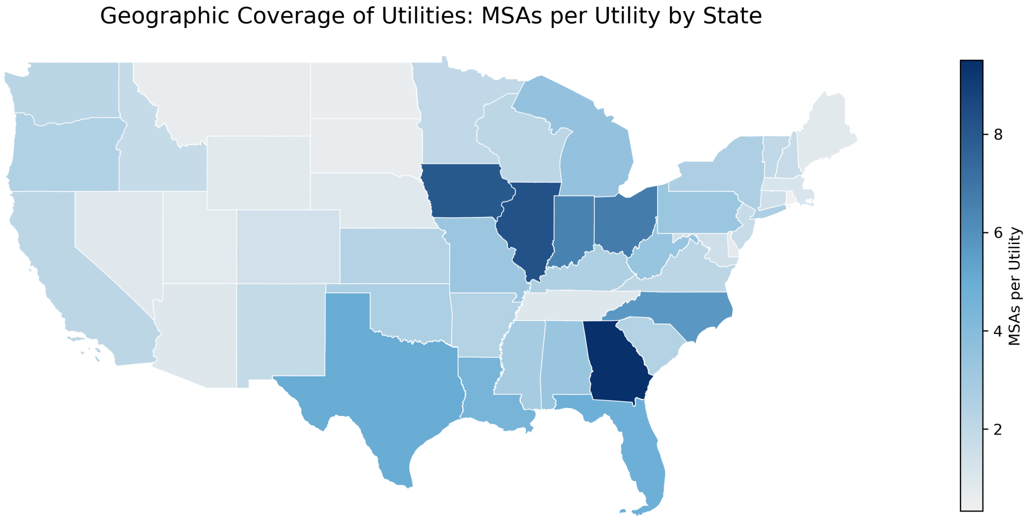

Figure 1: Geographic Coverage of Utilities: MSAs per Utility by State

Note: Darker shades indicate that a single utility serves a larger number of MSAs within a state.

To construct MSA-level electricity consumption measures, I combine utility-level sales data with the Service Territory Information schedule from EIA Form 861, which identifies the counties served by each utility. I then allocate utility-level electricity sales across counties using county population weights and aggregate the resulting county-level estimates to the MSA level. As a robustness check, I also construct MSA-level electricity consumption using county employment shares from the County Business Patterns (CBP) as an alternative weighting scheme. The results are highly similar under both weighting approaches.

I.II Natural Disasters

The primary data sources for disaster events are the Storm Events Database maintained by NOAA's National Centers for Environmental Information (NCEI) and the Atlantic Hurricane Database (HURDAT2) provided by NOAA's National Hurricane Center

(NHC). I primarily focus on natural disasters for which wind speed data are available, using recorded wind speed as an objective measure of disaster intensity. In the Storm Events Database, event types such as high wind, marine high wind, marine strong wind, marine thunderstorm wind, strong wind, and thunderstorm wind include recorded wind speeds and are documented separately from tropical storms, hurricanes, tornadoes, floods, and hail. From the HURDAT2 database, I use sustained maximum wind speed associated with Atlantic hurricanes to measure disaster intensity. I exclude tornado events from the analysis because direct wind speed measurements are not available for tornadoes[4].

Using MSA-level monthly average wind speed, I construct an indicator for months in which average wind speed exceeds 96 mph, corresponding to the lower bound of a Category 2 hurricane and thus capturing events from Category 2 through Category 5. Table 1 reports the monthly frequency of exposure to high winds across Categories 1 through 5. Exposure declines sharply for Category 2 and above and disaster incidence remains broadly dispersed across months.

Table 1: Monthly Frequency of High-Wind Storms by Category 1–5 (2018–2024)

[4]Tornado intensity is classified using the Enhanced Fujita (EF) scale, which infers wind speed ranges based on observed post-event damage rather than direct measurements. Because these values are inferred rather than observed, I exclude tornado exposures from the analysis.

Month	Cat 1	Cat 2	Cat 3	Cat 4	Cat 5
Jan	54	6	1		
Feb	36	2	2		
Mar	44	2	1		
Apr	43	2			
May	25	1			
Jun	29	1			
Jul	27	1		1	
Aug	30	5	1	1	
Sep	23	3		1	
Oct	26	2	1	1	1
Nov	29	1			
Dec	46	2	1		
Total	412	28	7	4	1

I.III City Concentration Characteristics

I construct three key pre-period measures using 2017 data to capture different dimensions of urban agglomeration. First, I calculate the Herfindahl–Hirschman Index (HHI) of industrial composition to capture the concentration of employment across industries within a city. Second, to capture overall road network centrality, I compute the Mean Edge Betweenness Centrality ($wMEBC$), weighted by observed commuting patterns. $wMEBC$ measures the average importance of roads in channeling traffic flows within the network for required on-site workers. Finally, from the perspective of city-level goods sourcing, I construct the Intra-city Trade Flow Ratio ($IntraTFR$), which measures the extent to which a city relies on internal sourcing of goods.

Labor Market Job Concentration

First, regarding industrial composition, the key question is how concentrated employment is across industries within a city. The Herfindahl-Hirschman Index (HHI) of the labor market, constructed from industry-specific employment counts, measures the degree of employment concentration across industries within a city. MSA-month-industry-wise job counts are from the Quarterly Census of Employment and Wages (QCEW), which provides industry-specific employment data classified under the North American Industry Classification System (NAICS). Offered job counts are summarized at the NACIS code 4 digits, industry group level. As a result, the HHI of the labor market is defined as follows:

$$
\begin{aligned}
HHI_{c,m,y} &= \sum_{i=1}^{N} s_{i,c,m,y}^2 \\
&= \sum_{i=1}^{N} \left(\frac{J_{i,c,m,y}}{J_{c,m,y}}\right)^2
\end{aligned}
\tag{1}
$$

where N represents the total number of industries in city c, $s_{i,c}^2$ represents the employment share of industry i in city c, month m and year y. To be more specific, $J_{i,c,m,y}$ represents the number of jobs in industry i and $J_{c,m,y}$ represents the total number of jobs across all industries.

For the MSA-month level HHI, I use the 2017 average, which ranges from 0 to 1, with higher values indicating greater industry concentration and lower job diversity. For instance, Midland MSA in Texas has the second-highest average HHI among all cities, reflecting a highly concentrated labor market with limited occupational diversity. This is because over 50 percent of Midland's workforce is employed in the oil and gas industry and its related sectors.[5]

Road Network Concentration

Concerning the road network, I represent road segments as edges and intersections as network nodes, allowing the importance of individual road segments to be evaluated according to their role in connecting locations throughout the network (Marshall (2016)(46)). A representative measure widely used in the transportation (Sakakibara et al. (2004)) and social network (Qi et al. (2017)) literature is Edge Betweenness Centrality (EBC), which measures the extent to which a road segment lies on the shortest paths between pairs of locations. Road segments with higher EBC are more critical to efficient travel because fewer alternative shortest routes exist. For example, if a road segment provides the only

[5] Midland MSA is home to major oil companies, including EOG Resources, Concho Resources, Pioneer Natural Resources, Chevron, Shell, ExxonMobil, and Occidental Petroleum.

shortest path connecting two locations, its disruption forces travelers onto longer routes, reducing the efficiency of movement within the network. Thus, higher edge betweenness centrality indicates that a road segment lies on a larger share of shortest paths between locations, implying that its disruption is more likely to create bottlenecks and reduce travel efficiency.

In addition to the physical structure of the road network, recent literature highlights the role of commuting patterns in shaping localized economic outcomes (Monte et al. (2018)(51)[6]). Workers in on-site occupations that are difficult to perform remotely must rely on the road network to access their workplaces, whereas workers in telecommutable occupations, such as financial services, face substantially weaker commuting constraints. Recognizing that commuting burdens vary with occupational composition, I extend the $MEBC$ measure to incorporate the commuting patterns of workers who are physically required to work on site. Under this framework, weighted road network centrality reflects the extent to which an MSA's transportation network depends on a small number of critical road segments for commuting.

Census block level commuting patterns by occupation are drawn from the LEHD Origin Destination Employment Statistics (LODES), which provide home-workplace block pairs across three industry classifications: (1) goods-producing, (2) trade, transportation, and utilities, and (3) all other services. On average, an MSA contains roughly 20,000 to 30,000 census blocks, although this average masks substantial heterogeneity across cities[7]. Specifically, I treat each MSA as the final workplace destination for commuters. Within an MSA, each commuter arrives at a workplace located in a census block. For each census block, I observe the occupational composition of arriving commuters and use this information to weight road network centrality by the share of workers who are physically constrained to work on site. Among various occupations, I classify jobs in goods-producing industries, trade, transportation, and utilities as more physically constrained to the worksite[8]. This classification enables the measure to capture heterogeneity

[6]Monte et al. (2018)(51) show that variation in commuting patterns serves as an adjustment margin through which the localized effects of shocks are redistributed across space. In particular, heterogeneous commuting patterns across counties play a key role in shaping local employment responses to labor demand shocks.

[7]Small MSAs typically contain about 3,000 to 10,000 blocks, mid sized MSAs contain approximately 10,000 to 30,000 blocks, and large MSAs such as Los Angeles, New York, or Dallas Fort Worth can include well over 100,000 census blocks, in some cases exceeding 300,000.

[8]In contrast, less physically constrained occupations include producer services such as finance, insurance, and arts-related activities. Although this classification is not without limitations, as some

in commuting intensity and physical presence requirements across occupations.

Based on this concept, I construct a commuting pattern adjusted road-network centrality at the block level. To compute topological indices, I use road networks obtained from OpenStreetMap (OSM) using the OSMnx module in Python (Boeing, 2017a (10)). Let b index workplace census blocks, and let $\mathcal{B}_c$ denote the set of workplace blocks located in MSA c. I begin by assigning to each block b a measure of road-network centrality derived from the metropolitan road network N_c.

$EBC_b(N_c)$ denote the block-assigned road-network centrality, defined as the average edge-betweenness centrality of road segments in the metropolitan road network N_c that are spatially associated with workplace block b:

$$EBC_b(N_c) = \frac{1}{|E_b(N_c)|} \sum_{e \in E_b(N_c)} EBC(e; N_c), \tag{2}$$

where $E_b(N_c) \subseteq E(N_c)$ denotes the set of road segments in N_c assigned to block b through the spatial overlay procedure.

Using this block-level assignment, I construct a commute-adjusted measure of road-network exposure at the block level:

$$wEBC_b = EBC_b(N_c) \cdot \text{Share}_b^{HP}, \tag{3}$$

where

$$\text{Share}_b^{HP} = \frac{\sum_o \sum_{s \in \mathcal{S}^{HP}} OD_{o \to b,s}}{\sum_o \sum_{s \in \mathcal{S}} OD_{o \to b,s}} \tag{4}$$

is the share of commuters to block b employed in sectors with high physical-presence requirements. Here, $OD_{o \to b,s}$ denotes the number of workers commuting from origin block o to workplace block b in industry sector s; $\mathcal{S}$ is the set of all industry sectors; and $\mathcal{S}^{HP} \subseteq \mathcal{S}$ denotes sectors that are, on average, more tightly bound to on-site work.

Finally, I aggregate the block-level measure to the metropolitan level by taking a share-weighted average across workplace blocks:

$$wMEBC_c = \frac{\sum_{b \in \mathcal{B}_c} EBC_b(N_c) \cdot \text{Share}_b^{HP}}{\sum_{b \in \mathcal{B}_c} \text{Share}_b^{HP}}. \tag{5}$$

physically constrained sectors such as accommodation, health, and education are also included in this category, it remains reasonable to treat this group as relatively less constrained than strictly on-site occupations.

As a result, the onsite-commuting constrained $MEBC$, $wMEBC$, is a time-invariant measure between 0 and 1, where higher values indicate that commuting flows for on-site workers are concentrated on a small number of critical road segments, rendering the network more susceptible to bottlenecks. Road segments that are crucial for connecting locations within the city, therefore, reflect the extent to which city operations may be disrupted by traffic accidents, road construction, or severe weather conditions (Mattsson et al. (2015)(47)).

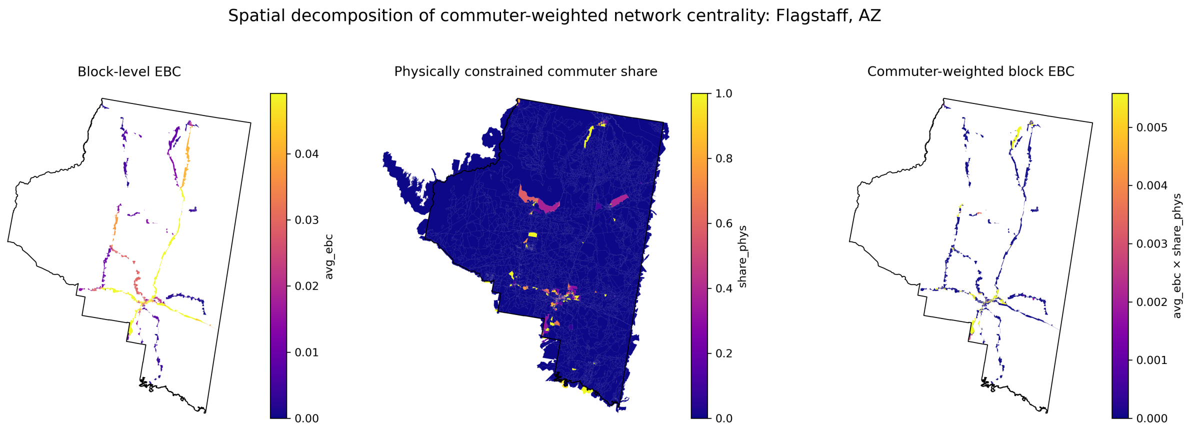

Figure 2: Highest $wMEBC$: Flagstaff, AZ

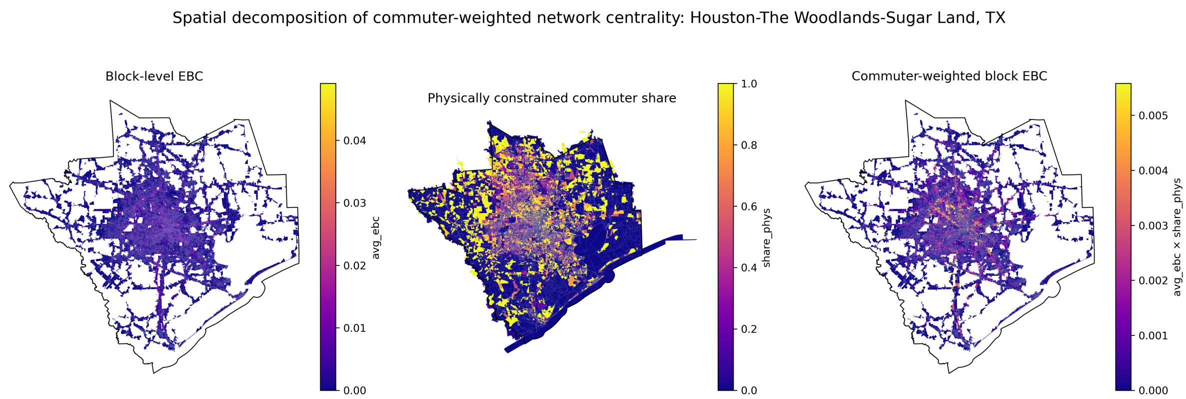

Figure 3: Lowest $wMEBC$: Houston-Sugar Land-Baytown, TX

Figure 2 presents Flagstaff, Arizona, which has the highest $wMEBC$. First, Flagstaff's road network is highly constrained, with only a few primary corridors. As a result, a small number of locations carry a disproportionately large share of shortest-path traffic. Along with this structural configuration, commuter flows in Flagstaff also display a similar pattern of concentration. with physically constrained commuting largely occurring along these same corridors rather than being dispersed across the network. The alignment between network centrality and commuter flows leads to a pronounced amplification effect in $wMEBC$. As a result, high $wMEBC$ values are spatially concentrated, indicating that the system depends heavily on a limited set of critical links, particularly for workers constrained to on-site locations.

In contrast, Figure 3 presents the MSA with the lowest $wMEBC$, Houston–Sugar Land–Baytown, TX. This region exhibits a highly distributed road network structure, indicating strong connectivity and the presence of numerous alternative routes. This configuration produces a relatively diffuse pattern of block-level betweenness centrality, with values distributed across many locations rather than concentrated in a few key nodes. In addition, commuter flows are similarly dispersed, with physically constrained commuting occurring across a broad spatial extent of the area. Because commuter activity is not strongly aligned with a limited set of high-centrality corridors, the interaction between network structure and commuting patterns does not generate strong localized amplification. Consequently, $wMEBC$ remains relatively low and spatially diffuse.

Intra-city Goods Trade Flow Concentration

Lastly, the flow of supplied goods plays a pivotal role in sustaining a city's economic activity. I construct a measure of goods flow concentration, the intra-city traded flow ratio ($IntraTFR$), which captures the relative importance of internally sourced trade linkages. Specifically, $IntraTFR$ reflects the extent to which goods delivered to city c are sourced from within the same city, relative to all metro-origin shipments delivered to that city.

The Freight Analysis Framework Version 5 (FAF5) Experimental County-Level Estimates, provided by the Bureau of Transportation Statistics, offer freight flow information by transportation mode and commodity group. While FAF5 reports shipment estimates at a coarser geographic level, an experimental county-level disaggregation factor, available only for 2022, is used to approximate county-to-county truck flows. To construct the pre-period $IntraTFR$ measure, I assume that the 2022 county-level disaggregation factors are unchanged from 2017. Applying this disaggregation factor, I first construct county-pair shipment volumes and then aggregate them to the MSA-pair level. In this step, I take the average shipment volume across all county pairs within each origin-MSA, destination-MSA, and commodity-group cell, capturing the average intensity of trade linkages between MSAs. I then aggregate these MSA-pair trade intensities across commodity groups to construct a city-level measure.

Based on this, the Intra-city Traded Flow Ratio ($IntraTFR$) is defined as follows:

$$IntraTFR_{c,y} = \frac{\sum_{j=c} T_{j\to c,y}}{\sum_j T_{j\to c,y}} \tag{6}$$

where $T_{j\to c,y}$ denotes the MSA-to-MSA shipment intensity from origin MSA j to destination MSA c in year y, constructed from average county-to-county shipment volumes within each MSA pair and aggregated across commodity groups. Accordingly, $\sum_{j=c} T_{j\to c,y}$ captures the inward trade intensity sourced from within MSA c, while $\sum_j T_{j\to c,y}$ captures the total inward trade intensity from all metro origins.

Figure 4 examines whether the three urban structural measures, HHI, $wMEBC$, and $IntraTFR$, capture distinct dimensions of urban structure. They are only weakly correlated, and none exhibits a high degree of overlap with the others, suggesting that each captures a different aspect of a city's economic structure. The strongest relationship is a moderate negative correlation of -0.46 between road network centrality and intra-city goods sourcing. This suggests that cities with more centralized road networks tend to rely less on intra-city goods sourcing, although the relationship remains moderate in magnitude.

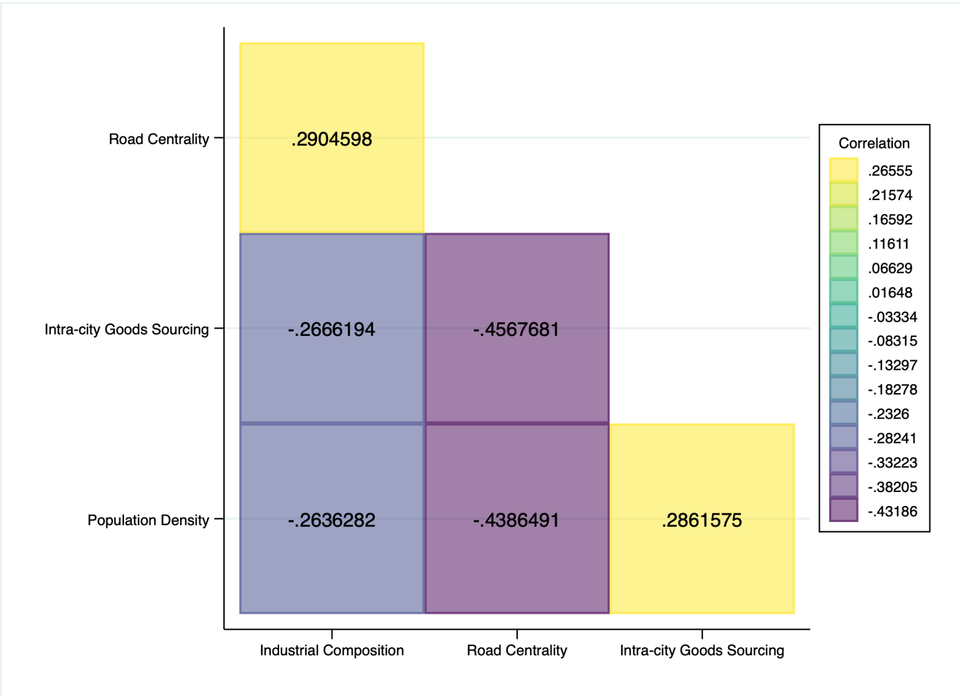

Figure 4: Correlation Matrix of Agglomeration Measures at the MSA Level

Figure 5 presents the MSA-level standardized pre-period measures of city concentration, enabling direct comparisons across cities. The raw measures are shown in Appendix Figure 7. The standardized results indicate pronounced geographic heterogeneity across MSAs.

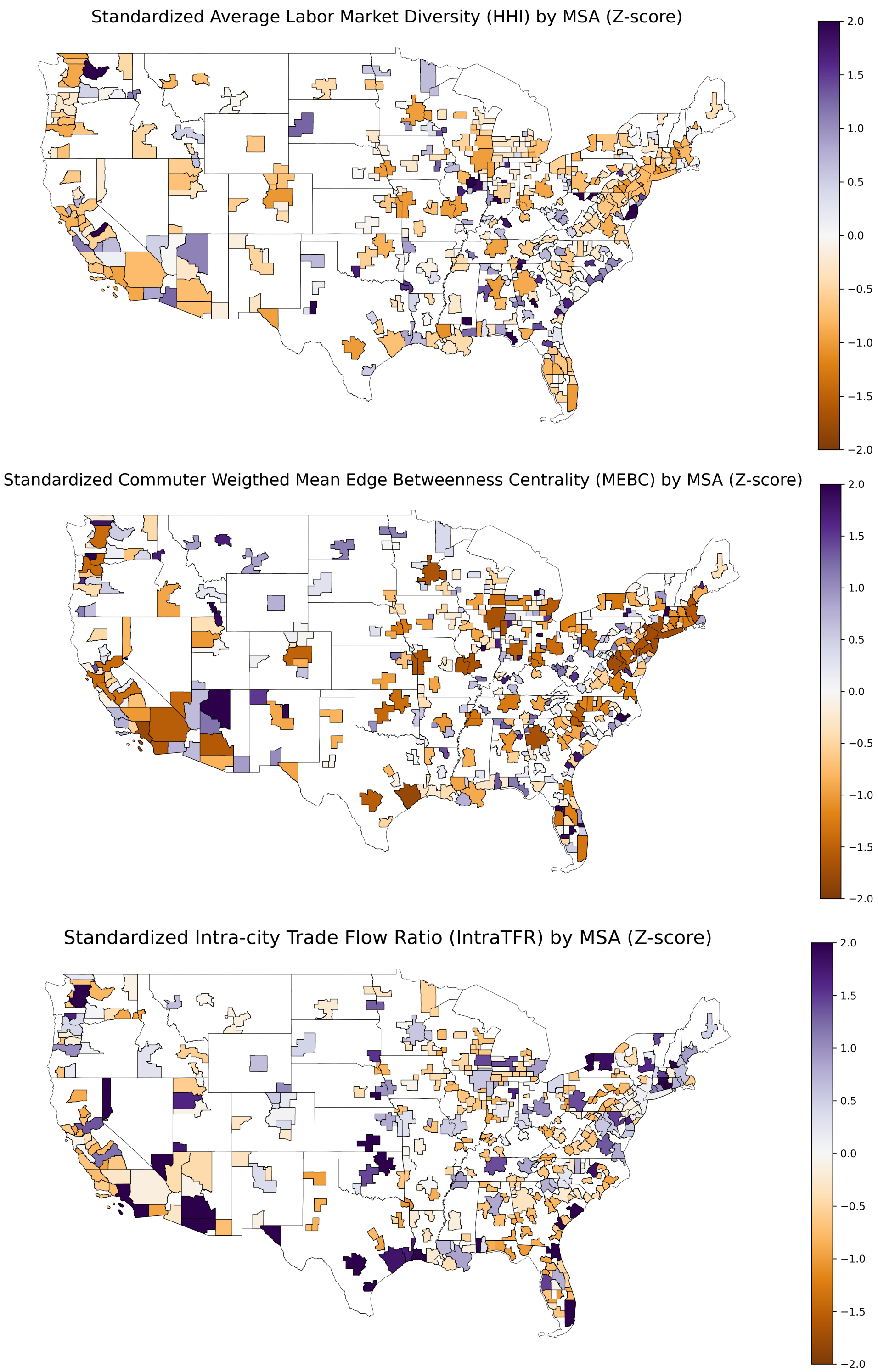

Figure 5: City-Level Concentration Measures (2017–2021): Standardized Z-Scores

Note: This figure presents the standardized Z-scores of average concentration measures for the labor market, road network, and trade perspectives across MSAs from 2017, allowing for cross-variable comparison.

II Research Design

II.I LP-DiD for Transient Natural Disasters

I begin by leveraging monthly high-wind disaster exposure across MSAs to examine how the economic disruption caused by natural disasters varies with urban concentration characteristics. In this context, the exogenous timing and location of disaster events provide plausibly exogenous variation for estimating the causal impact of disaster exposure interacted with concentration features. However, the discrete and episodic nature of disaster events complicates the construction of sustained treatment status and the identification of clean control groups. Because events are short-lived and occur intermittently, exposure in one month may be followed by new shocks in subsequent months, affecting both previously treated and untreated cities. This pattern can blur treatment timing and complicate the identification of clean comparison periods. Unlike policy interventions or structural reforms, which tend to remain in place for extended periods, natural disasters are transient events that switch on and off and may recur within the same MSAs. From this perspective, the classical two-way fixed effects framework may be biased due to the compounding effects of recurring shocks across cities. Even staggered difference-in-differences (DiD) methods do not fully address this issue, as they implicitly assume that treatment status persists over time, as in the case of policy interventions (De Chaisemartin et al. (2020)(20); Callaway et al. (2021)(14); Goodman-Bacon (2021)(34); Sun et al. (2021); Borusyak et al. (2024)(12)).

A key challenge is the need to identify valid treated and control MSAs. To address this, I apply the Local Projection-DiD method proposed by Dube et al. (2023)(22) and Jordà et al. (2025)(40), which is specifically designed to handle staggered treatment timing and dynamic treatment effects. The LP-DiD framework is particularly well-suited for capturing the dynamics of short-lived, non-persistent natural disasters. For instance, it accommodates cases where an MSA is hit in month m but not in the following month $m + 1$, allowing for shifts in treatment status. Specifically, under the LP-DiD approach, I construct valid samples by retaining each MSA first exposed to a disaster in month t that remains treated through the post period of interest, denoted by $t + h$. I then pair it with MSAs that have not experienced a disaster over the overlapping window from

$t-2$ to $t+h$[9]. A city is considered validly treated only if it is newly hit by a natural disaster in month t. In other words, I exclude MSAs that were hit in the previous month but are no longer treated in the current month to ensure stable treatment classification and to isolate the causal effect of disaster exposure from transitional dynamics. For each post-disaster month h, I construct period-specific samples and restrict the estimation to MSAs that remain in the corresponding sample.

Even when employing LP-DiD to mitigate issues of contaminated controls, concerns can persist regarding whether the selected control MSAs are truly comparable to treated cities in the context of natural disasters. Table 2 compares pre-period hurricane exposure across treated and control observations in the estimation sample. The results show that treated MSAs have higher pre-period maximum wind speed, while control observations have slightly higher pre-period average wind speed. However, neither difference is statistically significant, suggesting no systematic difference in baseline storm exposure across the two groups.

Table 2: Pre-period Hurricane Exposure in Treated and Control MSA-Month Observations

	Control		Treated			
Variable	Mean	SD	Mean	SD	Diff.	p-value
Pre-period Maximum Wind Speed	53.1541	23.3303	59.4286	30.2531	-6.2745	0.1119
Pre-period Average Wind Speed	19.7179	15.5717	18.0573	14.2778	1.6606	0.5283
Obs	30,380		35			

Note: This table reports pre-period hurricane exposure measures for the estimation sample at the MSA-month level. "Pre-period Maximum Wind Speed" is the maximum observed wind speed in a given MSA-month during the pre-period, while "Pre-period Average Wind Speed" is the corresponding average wind speed. The difference column reports Control minus Treated. P-values are from two-sample t-tests with equal variances.

The LP-DiD method is additionally advantageous in that it naturally accounts for past trends in the outcome variable, electricity consumption. Netting out the pre-trend of electricity consumption amounts is necessary to identify precisely the exact magnitude of each interaction's impact on short-run economic disruptions. Overall, the LP-DiD framework provides a credible and flexible approach for estimating the causal effects of

[9]For control cities, I require no-hit status beginning in (t-1) when matching them with treated cities, assuming that the economic effects of a disaster generally stabilize within one month regardless of disaster intensity. As a robustness check, I extend the stabilization window from one month to six months and find that the results remain highly consistent across specifications.

storm-related events by accommodating episodic on and off treatment status directly and accounting for pre-existing trends in electricity consumption.

Figure 6 presents the geographic distribution of the 24 treated MSAs from 2018 to 2024 identified under the LP-DiD framework. As expected, treated cities are largely located along coastal regions, particularly the Gulf Coast, with several inland cities being also included.

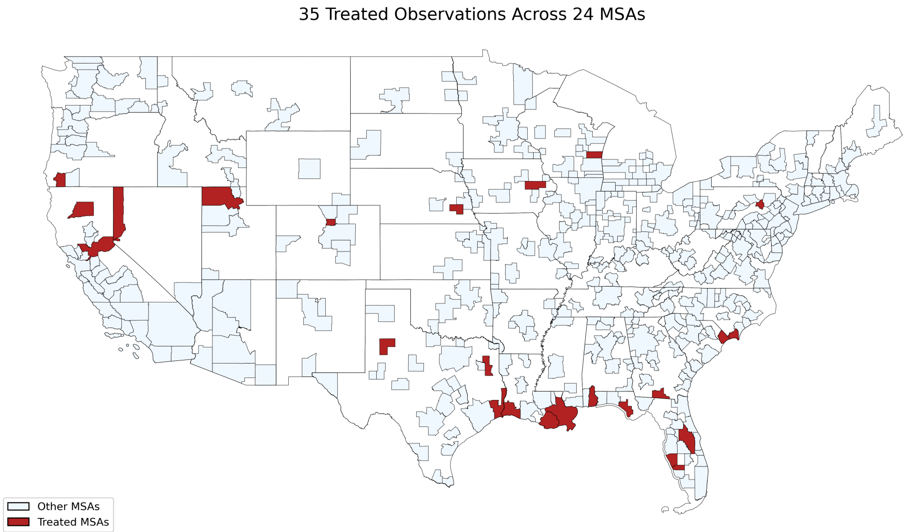

Figure 6: Geographic Distribution of Hit MSAs (2018-2024)

Note: The figure shows MSAs affected by natural disasters between 2018 and 2022 that experienced Category 2+ high-wind events (Saffir–Simpson scale). These MSAs are the treated units in the LP-DiD design.

II.II Econometric Framework

The adjusted estimating equation using the LP-DiD framework by Dube et al. (2023)(22) and Jordà et al. (2025)(40), with a primary focus on the heterogeneous effects of disaster exposure based on city concentration measures, takes the following form:

$$
\begin{aligned}
\ln(Load)_{c,m+h,y} - \ln(Load)_{c,m-1,y} = {} & (\delta_{m+h,y} - \delta_{m,y}) + \alpha_1 \, \Delta D_{c,m,y} \\
& + \Delta D_{c,m,y} \Big[\underbrace{\beta_1 \, HHI_c}_{\substack{\text{Labor Mkt:} \\ \text{ind. comp.}}} + \underbrace{\beta_2 \, wMEBC_c}_{\substack{\text{Road Net.:} \\ \text{central.}}} + \underbrace{\beta_3 \, IntraTFR_c}_{\substack{\text{Trade Flow:} \\ \text{goods sourcing}}} + \underbrace{\beta_4 \, PopDensity_c}_{\substack{\text{Urban form:} \\ \text{density}}} \Big] \\
& + \gamma_1 HDD_{c,m+h,y} + \gamma_2 CDD_{c,m+h,y} \\
& + \gamma_3 OutageCount_{c,m+h,y} + \gamma_4 BuildingSh_{\text{Pre-2000},c,y} \\
& + \epsilon_{c,m+h,y} \qquad (7)
\end{aligned}
$$

In Equation 7, c denotes the MSA, m denotes month, h denotes post horizon with $h \geq 0$ and y denotes the calendar year from 2018 to 2022. Equation 7 excludes region fixed effects but instead includes month-by-year fixed effects following the LP-DiD method. The outcome variable, $\ln(Load)_{c,m+h,y} - \ln(Load)_{c,m-1,y}$ captures the change in logged industrial and commercial electricity consumption h periods after a disaster, relative to the consumption level in the month prior to the natural disaster hit.

The variable $\Delta D_{c,m,y}$ equals one if MSA c is newly exposed in month m to high wind intensity equivalent to Saffir–Simpson Category 2 or above. Specifically, treatment is defined as one in the month an MSA is first struck by a high-intensity storm with maximum wind speeds exceeding 96 miles per hour.

$PopDensity$ is included to control for general city concentration intensity that may generate baseline differences in economic activities from the perspective of agglomeration forces. HDD and CDD represent heating and cooling degree days, respectively, measured at the MSA-month level, and are included to account for the influence of weather conditions on electricity consumption. The terms $(\delta_{m+h,y} - \delta_{m,y})$ capture time effects accounting for month-by-year fixed effects between the occurrence month and h periods ahead. Throughout the paper, standard errors are clustered at the MSA level to account for correlated shocks within each city, which may arise from disaster exposure patterns as well as from the structure of the sample. The coefficients of interest are from β_1 to β_3 which capture how disaster-driven impacts may be mitigated or amplified through each city's agglomeration measures.

Table 3 presents summary statistics on electricity consumption, agglomeration measures, and climatological variables during the disaster-occurring month, comparing MSAs affected by disasters to unaffected MSAs serving as control groups in the LP-DiD framework.

Table 3: Summary Statistics for Treated and Control MSAs

	Hit Cities		No-Hit Cities			
Variable	Mean	SD	Mean	SD	Diff.	p-value
Log Electricity Sales	12.613	1.223	12.119	1.276	-0.494	0.022
Road Network Centrality (Commuting Weighted)	0.013	0.007	0.014	0.006	0.001	0.452
Labor Market Concentration	0.042	0.018	0.045	0.025	0.003	0.467
Within-City Goods Sourcing Ratio	0.257	0.213	0.191	0.172	-0.066	0.023
CDD (thousands)	0.558	0.886	0.372	0.849	-0.186	0.196
HDD (thousands)	0.699	1.060	1.041	2.013	0.342	0.315
Obs	35		30,464			
MSAs	24		364			

Note: Summary statistics are reported at the onset month ($h = 0$), separately for MSAs newly exposed to high-wind disasters (Category 2 and above) and those not exposed. The table reports electricity sales, agglomeration measures, and climate controls at the time of initial exposure. The difference column reports (Control minus Treated).

III Results

Table 4 reports the average treatment effects of natural disasters of Saffir–Simpson Category 2 intensity or higher on broad changes in local economic activity. The estimated impact in the month of occurrence ($h = 0$), relative to the pre-disaster month, indicates an approximate 3 percent decline in overall economic activity. This estimate corresponds to an MSA evaluated at the average levels of the three agglomeration forces.

The subsequent rows report the heterogeneous slopes associated with each urban structural measure. All three dimensions exhibit statistically significant heterogeneity in shaping the economic impact of natural disasters. Greater industrial concentration, reflecting a higher concentration of employment in a small number of industries, significantly amplifies disaster-related economic losses. In contrast, stronger road network connectivity and greater intra-city goods sourcing concentration mitigate these adverse effects.

After establishing heterogeneity across the three agglomeration dimensions, I estimate treatment effects at different levels of each structural measure. This allows me to directly examine how the impacts of natural disasters vary across dimensions of urban economic structure. Specifically, I evaluate how the treatment effect of a natural disaster changes as each structural measure increases or decreases by one standard deviation from its sample

Category	Variable	Episodic Natural Disaster Changes in Monthly MSA Electricity Load Event Month ($h = 0$)
	Treatment effect	-0.0298^{***} (0.0058)
Labor Market	Industrial Composition (HHI)	-1.735^{***} (0.306)
Road Network	Road Connectivity ($wMEBC$)	3.410^{***} (0.906)
Trade Flow	Intra-city Goods Sourcing ($IntraTFR$)	0.0771^{***} (0.0284)
Demographics	Population Density	-0.000446^{***} (0.0000951)
	Observations	30,499

Note: Entries report marginal effects evaluated in the event month ($h = 0$) using population-based weights in constructing MSA-level electricity load. Standard errors are reported in parentheses and clustered at the MSA level. $^{***}p < 0.01$, $^{**}p < 0.05$, $^{*}p < 0.1$.

Table 4: Marginal Effects in the Event Month ($h = 0$): Category ≥ 2

mean, while holding the other two structural measures at their sample means.

Table 5 reports the estimated treatment effects evaluated at the sample mean and one standard deviation above and below the mean of each structural measure. The baseline corresponds to the treatment effect when all three structural measures are held at their sample means, and the remaining estimates capture the marginal effect of varying one structural dimension at a time.

For the industrial composition dimension, a one standard deviation increase in industrial concentration (HHI) from its mean substantially amplifies the adverse impact of natural disasters, reducing overall economic activity by approximately 7 percentage points relative to the mean. This represents the strongest gradient among the agglomeration forces considered, with a one standard deviation increase in concentration amplifying the treatment effect by a factor of about 2.5.

In contrast, for road connectivity, a one standard deviation increase in centrality ($wMEBC$) significantly mitigates disaster-related damages relative to a one standard deviation decrease. Under higher road network centrality, the estimated treatment effect is no longer statistically distinguishable from zero, suggesting that greater network centralization effectively buffers local economic losses. Similarly, greater concentration in intra city goods sourcing ($IntraTFR$) attenuates the negative impact of natural disasters. A one standard deviation increase in sourcing concentration reduces the magnitude of the treatment effect by approximately 44 percent relative to the average, indicating that more localized logistics networks enhance resilience to external shocks.

		Treatment Effects Across Urban Structure Levels			Baseline Effect
		Monthly Electricity Load			
Category	Variable	Low	High	Difference	
Labor Market	Industrial Composition (HHI)	0.0137 (0.0106)	-0.0734^{***} (0.0085)	-0.0872^{***} (0.0153)	-0.0298^{***} (0.0058)
Road Network	Road Connectivity ($wMEBC$)	-0.0514^{***} (0.0097)	-0.0083 (0.0062)	0.0432^{***} (0.0114)	
Trade Flow	Intra-city Goods Sourcing ($IntraTFR$)	-0.0430^{***} (0.0100)	-0.0166^{***} (0.0039)	0.0264^{***} (0.0097)	
Observations: 30,499					

Note: Low and High columns evaluate treatment effects at mean−sd and mean+sd of each urban structure measure. The Difference column reports High minus Low. The Baseline column reports the treatment effect evaluated at sample means. Standard errors are clustered at the MSA level. $^{***}p < 0.01$, $^{**}p < 0.05$, $^{*}p < 0.1$.

Table 5: Heterogeneous Treatment Effects by Urban Structure Intensity

IV Heterogeneity by Sectoral Specialization

Results from Section III show that urban economic structure can either amplify or mitigate the economic impacts of natural disasters. Among the three dimensions examined, industrial concentration uniquely amplifies disaster damages and generates the largest variation in treatment effects. This prominent role of industrial concentration relates closely to a well-established body of evidence attributing recent urban growth to productivity gains from specialization in professional services[10] (Caliendo et al., 2018; Eckert et al., 2022; Rossi-Hansberg et al., 2021[11]). While this literature has primarily emphasized the productivity and growth benefits of sectoral specialization, much less is known about its implications for cities' vulnerability to natural disasters. In particular, although recent urban growth has been driven by a narrow set of highly agglomerated sectors of business services and health and education, it remains unclear whether specialization in these sectors makes cities more resilient or more vulnerable to disaster-related disruptions. This

[10]The professional services sector includes NAICS codes 51–56, comprising Information (51), Finance and Insurance (52), Real Estate and Rental and Leasing (53), Professional, Scientific, and Technical Services (54), Management of Companies and Enterprises (55), and Administrative and Support and Waste Management and Remediation Services (56).

[11]For instance, Eckert et al. (2022) show that between 1980 and 2015, urban-biased wage growth originated almost entirely within business services, where the wage gap between high- and low-density areas widened substantially while remaining largely flat in other sectors.

motivates a closer examination of sectoral specialization as a mechanism through which industrial concentration shapes disaster resilience.

Accordingly, Section IV.I introduces an additional layer of analysis by incorporating industry group-specific specialization alongside the three structural measures. In particular, I examine whether the effect of industrial concentration on disaster damages depends on the industries in which a city specializes. Special attention is given to retail, utilities, and construction (RUC) and manufacturing, alongside business services, the sector most closely associated with productivity gains from geographic concentration.

IV.I Sectoral Specialization as an Additional Moderator

I follow the existing literature and group industries into five categories: Retail Trade, Utilities, and Construction (RUC); Health and Education (HE); Professional and Other Services (PS); Manufacturing (M); and Accommodation, Trade, and Transportation (ATT). I then examine whether MSAs that were more specialized in each group during the pre-period (2013 to 2017), as indicated by an above national average employment share, exhibit different resilience to natural disasters.

Equation 8 extends the baseline specification of agglomeration adjustment under natural disasters, Equation 7, by incorporating a measure of sectoral specialization relative to the national average, $(Sectsh_c - \overline{Sectsh})$. Here, $\overline{Sectsh}$ denotes the national average employment share across the five industry groups, while $Sectsh_c$ represents the corresponding MSA-specific employment share, both measured over the pre period. A positive value of $(Sectsh_c - \overline{Sectsh})$ indicates that MSA c is relatively specialized in that sector compared to the national benchmark.

$$
\begin{aligned}
\ln(Load)_{c,m+h,y} - \ln(Load)_{c,m-1,y} = {} & (\delta_{m+h,y} - \delta_{m,y}) + \alpha_1 \, \Delta D_{c,m,y} \\
& + \Delta D_{c,m,y} \times \left[\beta_1 \, HHI_c + \beta_2 \, MEBC_c + \beta_3 \, IntraTFR_c + \beta_4 \, PopDensity_c\right] \\
& + \Delta D_{c,m,y} \times (SectSh_c - \overline{SectSh}) \times \left[\beta_1 \, HHI_c + \beta_2 \, wMEBC_c + \beta_3 \, IntraTFR_c + \beta_4 \, PopDensity_c\right] \\
& + \gamma_1 HDD_{c,m+h,y} + \gamma_2 CDD_{c,m+h,y} \\
& + \gamma_3 OutageCount_{c,m+h,y} + \gamma_4 BuildingSh_{\text{Pre-2000},c,y} \\
& + \epsilon_{c,m+h,y} \qquad (8)
\end{aligned}
$$

Table 6 reports how the effect of exposure to Category 2 and above natural disasters on economic activity in the month of impact varies with the degree of specialization in retail, utilities, and construction (RUC), business services, and manufacturing, while holding the three urban structural measures at their sample means. The results indicate that MSAs with greater specialization in retail, utilities, and construction experience substantially larger disaster-related declines in economic activity than less specialized MSAs. A similar pattern is observed for manufacturing specialization, although the estimated effects are less stable across specifications. In contrast, no comparable pattern emerges for business services. Overall, these findings suggest that the vulnerability associated with industrial concentration depends on the sector in which a city specializes, with specialization in RUC playing a particularly important role in amplifying disaster-related economic losses.

	RUC + BS + Manu			Statistical Diff.
Sector	Below	Average	Above	Difference
RUC	-0.017	-0.037***	-0.057***	-0.040**
Manufacturing	0.007	-0.037***	-0.081***	-0.088*
Business Service	-0.039**	-0.037***	-0.035***	0.004

Note: Entries report marginal treatment effects evaluated at -1, 0, and $+1$ standard deviations of sectoral specialization. The Difference column reports the difference between treatment effects evaluated at $+1$ and -1 standard deviations of specialization. Standard errors are clustered at the MSA level. $^{***}p < 0.01$, $^{**}p < 0.05$, $^{*}p < 0.1$.

Table 6: Heterogeneous Treatment Effects by Sectoral Specialization

V Conclusion

Despite the huge emphasis on urban agglomeration intensity as a critical driver of growth, little empirical work has explored how they may differentially shape the economic impacts of natural disasters. Considering the localized nature of most natural disasters, this remains a striking gap in understanding the full range of their economic effects. Since various concentration conditions can shape the realized impacts from natural disasters differently and can also have different levels of lingering impacts, they should be taken into consideration for a comprehensive assessment of disaster-induced economic disruptions at the city level.

Investigating the interaction between natural disasters and urban economic structure also helps identify more effective directions for disaster risk-reduction investments, particularly because urban development decisions often prioritize economic gains over potential disaster risks.[12] The importance of this issue is further heightened as natural disasters become increasingly severe while remaining inherently unpredictable. Because local governments shape disaster vulnerability through infrastructure investment, land-use regulation, and resilience planning, understanding how city-specific concentration structures amplify or mitigate disaster-induced disruptions can help guide more effective ex-ante risk-reduction strategies. For example, research emphasizing the high long-term costs of coastal road investments under accelerating climate change (Balboni (2025)(3) gains an additional dimension when recognizing that the short-run economic consequences of disasters also depend on how shocks interact with a city's underlying economic structure. More broadly, understanding these trade-offs allows cities to be evaluated not only by the economic opportunities generated through concentration, but also by their resilience to natural disasters.

[12]For instance, Lin et al. (2024)(43) show that, despite awareness of rising sea levels, people continued to move into coastal U.S. cities between 1990 and 2010 to capture the economic benefits of urban proximity. This highlights a broader tendency to accept disaster-related risks in exchange for economic opportunities.

VI Appendix

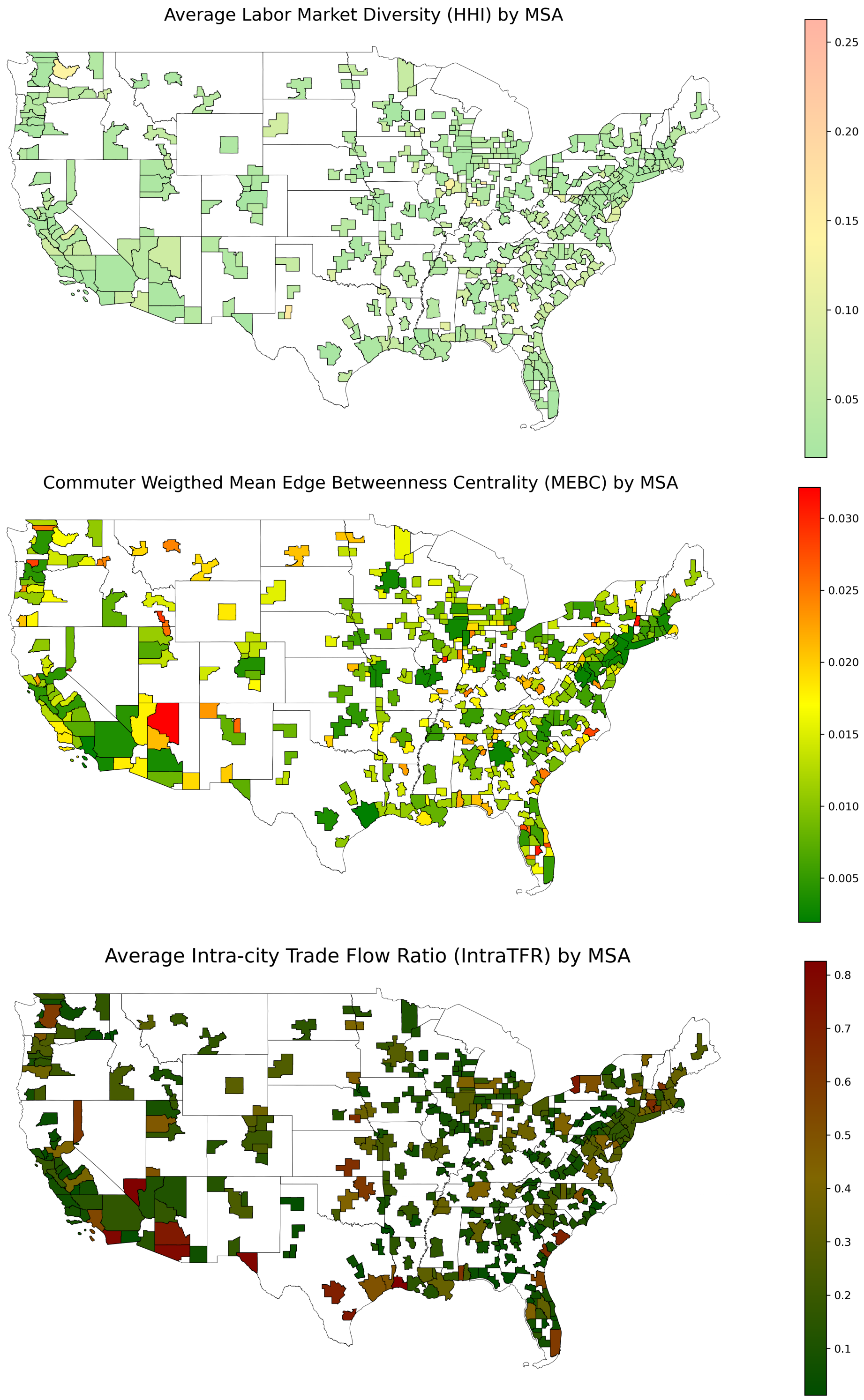

Figure 7: City-Level Concentration Measures (2017–2021)

Note: This figure presents average concentration measures for the labor market, road network, and trade perspectives across MSAs from 2017.

Table 7: Dynamic Marginal Effects on QCEW Employment Changes and Growth Rates

		Episodic Natural Disaster					
		Employment Change			Employment Growth		
Category	Variable	Event Month ($h = 0$)	One Month After ($h = 1$)	Two Months After ($h = 2$)	Event Month ($h = 0$)	One Month After ($h = 1$)	Two Months After ($h = 2$)
Panel A. One-Month Employment Outcomes							
Treatment Effect		-1.646^{**}	-2.235	1.746^{**}	-0.00565^{*}	-0.00282	0.00886^{***}
		(0.738)	(1.488)	(0.767)	(0.00342)	(0.00380)	(0.00216)
Labor Market	Industrial Composition (HHI)	-57.871^{*}	10.060	45.695^{*}	-0.241	-0.00391	0.386^{***}
		(32.688)	(41.137)	(25.739)	(0.273)	(0.261)	(0.106)
Road Network	Road Connectivity ($wMEBC$)	71.032	199.396	-115.940	-0.248	-1.547	0.242
		(87.738)	(137.938)	(75.668)	(0.412)	(0.942)	(0.377)
Trade Flow	Intra-city Goods Sourcing ($IntraTFR$)	2.774	-9.566	0.0811	0.0108	-0.0784	-0.00482
		(4.330)	(6.574)	(2.342)	(0.0195)	(0.0513)	(0.00736)
Demographics	Population Density	-0.0253^{**}	0.00360	0.0310^{***}	-0.0000109	0.0000810	0.00000935
		(0.0115)	(0.0301)	(0.00924)	(0.0000473)	(0.0000810)	(0.0000282)
Panel B. Two-Month Average Employment Outcomes							
Treatment Effect		-1.027^{**}	-2.219^{***}	-0.515	-0.00378^{*}	-0.00523^{*}	0.00204
		(0.439)	(0.584)	(0.600)	(0.00227)	(0.00294)	(0.00203)
Labor Market	Industrial Composition (HHI)	-34.850^{*}	-27.722	22.500	-0.152	-0.153	0.159
		(20.949)	(28.448)	(21.615)	(0.195)	(0.247)	(0.149)
Road Network	Road Connectivity ($wMEBC$)	-43.754	54.142	-30.072	-0.131	-0.905	-0.649^{**}
		(56.165)	(84.215)	(59.941)	(0.221)	(0.572)	(0.297)
Trade Flow	Intra-city Goods Sourcing ($IntraTFR$)	1.988	-2.730	-4.208^{*}	0.0116	-0.0275	-0.0355^{**}
		(1.563)	(3.000)	(2.189)	(0.00774)	(0.0271)	(0.0180)
Demographics	Population Density	-0.0248^{***}	-0.0239^{**}	0.00440	-0.0000180	0.0000221	0.0000323
		(0.00841)	(0.00978)	(0.0104)	(0.0000258)	(0.0000428)	(0.0000304)
Panel C. Three-Month Average Employment Outcomes							
Treatment Effect		-0.877^{**}	-1.848^{***}	-1.241^{**}	-0.00203	-0.00371	-0.000742
		(0.371)	(0.537)	(0.527)	(0.00167)	(0.00233)	(0.00234)
Labor Market	Industrial Composition (HHI)	-37.507^{*}	-35.610	-20.647	-0.147	-0.167	-0.0383
		(22.426)	(33.510)	(28.108)	(0.137)	(0.201)	(0.203)
Road Network	Road Connectivity ($wMEBC$)	68.968^{**}	80.444	38.733	0.175	-0.348	-0.269
		(31.092)	(61.029)	(56.746)	(0.201)	(0.314)	(0.242)
Trade Flow	Intra-city Goods Sourcing ($IntraTFR$)	1.638^{*}	-1.072	-1.018	0.0135^{**}	-0.00837	-0.00995
		(0.966)	(1.696)	(1.537)	(0.00557)	(0.0117)	(0.0109)
Demographics	Population Density	-0.0227^{***}	-0.0307^{***}	-0.0200^{***}	-0.0000171	0.000000240	0.00000360
		(0.00500)	(0.00710)	(0.00699)	(0.0000173)	(0.0000257)	(0.0000242)
	Observations	30,104	29,714	29,323	30,104	29,714	29,323

Notes: Entries report marginal effects on changes in QCEW MSA employment outcomes following average Category ≥ 2 storm exposure. Within each panel, the first three columns report results for absolute employment-change measures, while the final three columns report results for log employment-growth measures.

Panel A uses one-month measures. The absolute employment-change measure is defined as $E_{it} - E_{i,t-1}$, and the log employment-growth measure is defined as $\ln(E_{it}) - \ln(E_{i,t-1})$. Panel B uses two-month average measures, defined as $(E_{it} - E_{i,t-2})/2$ and $[\ln(E_{it}) - \ln(E_{i,t-2})]/2$. Panel C uses three-month average measures, defined as $(E_{it} - E_{i,t-3})/3$ and $[\ln(E_{it}) - \ln(E_{i,t-3})]/3$.

Employment levels used to construct the absolute-change measures are measured in thousands of employees. Log-growth estimates are expressed in log points; multiplying them by 100 gives approximate percentage-point effects. At each horizon h, the LP–DiD outcome compares the corresponding employment-change or employment-growth measure in month $t + h$ with its value in month $t - 1$.

Treatment is defined by an eligible storm onset in the event month ($h = 0$). The same event-month treatment assignment is used at all subsequent horizons, so estimates at $h > 0$ trace the dynamic response following the initial storm event without requiring treatment status to remain unchanged after the event month. Control MSAs are required to exhibit no treatment-status transitions during the relevant pre-event stabilization window. The stabilization window is two months for $h = 0$, three months for $h = 1$, and four months for $h = 2$.

Standard errors are reported in parentheses and clustered at the MSA level. Electricity-specific controls, including HDD, CDD, the share of pre-1980 housing stock, and outage measures, are excluded. $^{***}p < 0.01$, $^{**}p < 0.05$, $^{*}p < 0.1$.

References

[1] Allen, T., & Arkolakis, C. (2022). The welfare effects of transportation infrastructure improvements. The Review of Economic Studies, 89(6), 2911-2957.

[2] Bakker, J. D., Marin, A. G., Potlogea, A. V., Voigtländer, N., & Yang, Y. (2024). Cities, heterogeneous firms, and trade (No. w32377). National Bureau of Economic Research.

[3] Balboni, C. (2025). In harm's way? Infrastructure investments and the persistence of coastal cities. American Economic Review, 115(1), 77–116.

[4] Barrero, J. M., Bloom, N., & Davis, S. J. (2021). Why working from home will stick (No. w28731). National Bureau of Economic Research.

[5] Barrot, J. N., & Sauvagnat, J. (2016). Input specificity and the propagation of idiosyncratic shocks in production networks. The Quarterly Journal of Economics, 131(3), 1543-1592.

[6] Baum-Snow, N. (2007). Did highways cause suburbanization? The Quarterly Journal of Economics, 122(2), 775–805.

[7] Behrens, K., Duranton, G., & Robert-Nicoud, F. (2014). Productive cities: Sorting, selection, and agglomeration. Journal of Political Economy, 122(3), 507–553.

[8] Bergantino, A. S., Gardelli, A., & Rotaris, L. (2024). Assessing transport network resilience: empirical insights from real-world data studies. Transport Reviews, 44(4), 834-857.

[9] Boehm, C. E., Flaaen, A., & Pandalai-Nayar, N. (2019). Input linkages and the transmission of shocks: Firm-level evidence from the 2011 Tōhoku earthquake. Review of Economics and Statistics, 101(1), 60–75.

[10] Boeing, G. (2017a). OSMnx: A Python package to work with graph-theoretic OpenStreetMap street networks. Journal of Open Source Software, 2(12), 215.

[11] Boeing, G. (2017b). OSMnx: New methods for acquiring, constructing, analyzing, and visualizing complex street networks. Computers, Environment and Urban Systems, 65, 126–139.

[12] Borusyak, K., Jaravel, X., & Spiess, J. (2024). Revisiting event-study designs: Robust and efficient estimation. Review of Economic Studies, 91(6), 3253–3285.

[13] Caliendo, L., Parro, F., Rossi-Hansberg, E., & Sarte, P. D. (2018). The impact of regional and sectoral productivity changes on the US economy. The Review of economic studies, 85(4), 2042-2096.

[14] Callaway, B., & Sant'Anna, P. H. (2021). Difference-in-differences with multiple time periods. Journal of Econometrics, 225(2), 200–230.

[15] Carvalho, V. M., Nirei, M., Saito, Y. U., & Tahbaz-Salehi, A. (2021). Supply chain disruptions: Evidence from the great east japan earthquake. The Quarterly Journal of Economics, 136(2), 1255–1321.

[16] Casali, Y., & Heinimann, H. R. (2019). A topological characterization of flooding impacts on the Zurich road network. PLoS ONE, 14(7), e0220338.

[17] Cicala, S. (2023). JUE Insight: Powering work from home. Journal of Urban Economics, 133, 103474.

[18] Combes, P. P., Duranton, G., Gobillon, L., Puga, D., & Roux, S. (2012). The productivity advantages of large cities: Distinguishing agglomeration from firm selection. Econometrica, 80(6), 2543-2594.

[19] Cooper, R. W., & Haltiwanger, J. C. (2006). On the nature of capital adjustment costs. The Review of Economic Studies, 73(3), 611-633.

[20] De Chaisemartin, C., & d'Haultfoeuille, X. (2020). Two-way fixed effects estimators with heterogeneous treatment effects. American Economic Review, 110(9), 2964–2996.

[21] Dingel, J. I., & Neiman, B. (2020). How many jobs can be done at home?. Journal of public economics, 189, 104235.

[22] Dube, A., Girardi, D., Jordà, Ò., & Taylor, A. M. (2023). A local projections approach to difference-in-differences event studies (No. w31184). National Bureau of Economic Research.

[23] Duranton, G., & Puga, D. (2001). Nursery cities: urban diversity, process innovation, and the life cycle of products. American Economic Review, 91(5), 1454-1477.

[24] Duranton, G., & Turner, M. A. (2012). Urban growth and transportation. Review of Economic Studies, 79(4), 1407–1440.

[25] Duranton, G., Morrow, P. M., & Turner, M. A. (2014). Roads and Trade: Evidence from the US. Review of Economic Studies, 81(2), 681–724.

[26] Duranton, G., & Turner, M. A. (2011). The fundamental law of road congestion: Evidence from US cities. American Economic Review, 101(6), 2616-2652.

[27] Eckert, F., Ganapati, S., & Walsh, C. (2022). Urban-biased growth: a macroeconomic analysis (No. w30515). National Bureau of Economic Research.

[28] Fajgelbaum, P. D., & Schaal, E. (2020). Optimal transport networks in spatial equilibrium. Econometrica, 88(4), 1411-1452.

[29] Federal Highway Administration (FHWA)., Emergency Relief Manual (Federal-Aid Highways)., Office of Infrastructure, Office of Program Administration, Updated May 31, 2013.

[30] Gagliardi, L., Moretti, E., & Serafinelli, M. (2023). The world's rust belts: The heterogeneous effects of deindustrialization on 1,993 cities in six countries (No. w31948). National Bureau of Economic Research.

[31] Gentili, E. (2025). The impact on economic activity and housing market of the 2023 Emilia-Romagna floods (No. 1506). Bank of Italy, Economic Research and International Relations Area.

[32] Glaeser, E. L., Saiz, A., Burtless, G., & Strange, W. C. (2004). The rise of the skilled city [with comments]. Brookings-Wharton Papers on Urban Affairs, 47–105.

[33] Glaeser, E. L., Kallal, H. D., Scheinkman, J. A., & Shleifer, A. (1992). Growth in cities. Journal of political economy, 100(6), 1126-1152.

[34] Goodman-Bacon, A. (2021). Difference-in-differences with variation in treatment timing. Journal of Econometrics, 225(2), 254–277.

[35] Heblich, S., Nagy, D. K., Trew, A., & Zylberberg, Y. (2025). The death and life of great British cities (No. w34029). National Bureau of Economic Research.

[36] Holmes, T. J., & Stevens, J. J. (2002). Geographic concentration and establishment scale. Review of Economics and Statistics, 84(4), 682-690.

[37] Hsieh, C. T., & Rossi-Hansberg, E. (2023). The industrial revolution in services. Journal of Political Economy Macroeconomics, 1(1), 3-42.

[38] Jacobs, J. (1969). The economy of cities. Random House.

[39] Jarosch, G., Oberfield, E., & Rossi-Hansberg, E. (2021). Learning from coworkers. Econometrica, 89(2), 647-676

[40] Jordà, Ò., & Taylor, A. M. (2025). Local projections. Journal of Economic Literature, 63(1), 59–110.

[41] Korovkin, V., Makarin, A., & Miyauchi, Y. (2025). Supply chain disruption and reorganization: Theory and evidence from ukraine's war. Review of Economic Studies, rdaf080.

[42] Liao, Y., & Kousky, C. (2022). The fiscal impacts of wildfires on California municipalities. Journal of the Association of Environmental and Resource Economists, 9(3), 455–493.

[43] Lin, Y., McDermott, T. K., & Michaels, G. (2024). Cities and the sea level. Journal of Urban Economics, 143, 103685.

[44] Marin, A. G., Potlogea, A. V., Voigtländer, N., & Yang, Y. (2021). Cities, productivity, and trade (No. w28309). National Bureau of Economic Research.

[45] Marshall, A. (1890). Principles of economics, by Alfred Marshall (pp. 20-22). London: Macmillan and Company.

[46] Marshall, S. (2016). Line structure representation for road network analysis. Journal of Transport and Land Use, 9(1), 29–64.

[47] Mattsson, L. G., & Jenelius, E. (2015). Vulnerability and resilience of transport systems–A discussion of recent research. Transportation Research Part A: Policy and Practice, 81, 16–34.

[48] Miyauchi, Y. (2024). Matching and Agglomeration: Theory and Evidence From Japanese Firm-to-Firm Trade. Econometrica, 92(6), 1869-1905.

[49] Miyauchi, Y., Nakajima, K., & Redding, S. J. (2025). The economics of spatial mobility: Theory and evidence using smartphone data. The Quarterly Journal of Economics, 140(4), 2507-2570.

[50] Monte, F., Porcher, C., & Rossi-Hansberg, E. (2023). Remote work and city structure (No. w31494). National Bureau of Economic Research.

[51] Monte, F., Redding, S. J., & Rossi-Hansberg, E. (2018). Commuting, migration, and local employment elasticities. American Economic Review, 108(12), 3855-3890.

[52] Moretti, E., & Yi, M. (2024). Size matters: Matching externalities and the advantages of large labor markets (No. w32250). National Bureau of Economic Research.

[53] Redding, S. J., & Sturm, D. M. (2008). The costs of remoteness: Evidence from German division and reunification. American Economic Review, 98(5), 1766-1797.

[54] Rossi-Hansberg, E., Sarte, P. D., & Schwartzman, F. (2021, May). Local industrial policy and sectoral hubs. In AEA Papers and Proceedings (Vol. 111, pp. 526-531). 2014 Broadway, Suite 305, Nashville, TN 37203: American Economic Association.

[55] Rossi-Hansberg, E., Sarte, P. D., & Schwartzman, F. (2019). Cognitive hubs and spatial redistribution (No. w26267). National Bureau of Economic Research.

[56] Roth Tran, B., & Wilson, D. J. (2025). The local economic impact of natural disasters. Journal of the Association of Environmental and Resource Economists, forthcoming.

[57] Saiz, A. (2010). The geographic determinants of housing supply. The Quarterly Journal of Economics, 125(3), 1253-1296.

[58] Sun, L., & Abraham, S. (2021). Estimating dynamic treatment effects in event studies with heterogeneous treatment effects. Journal of Econometrics, 225(2), 175–199.

[59] Tachaudomdach, S., Upayokin, A., Kronprasert, N., & Arunotayanun, K. (2021). Quantifying road-network robustness toward flood-resilient transportation systems. Sustainability, 13(6), 3172.

[60] Tyndall, J. (2021). The local labour market effects of light rail transit. Journal of Urban Economics, 124, 103350.